Research Article

Siwen Tang*, Peizhen Li, Deshun Liu, Pengnan Li, and Qiulin Niu

Cutting performance of a functionally graded cemented carbide tool prepared by microwave heating and nitriding sintering

https://doi.org/10.1515/htmp-2019-0011
Received Mar 12, 2018; accepted Dec 25, 2018

Abstract: The cutting force, the friction coefficient of the rake face, and the flank wear of functional gradient cemented carbide (FGCC) cutting tools prepared by microwave heating and nitriding sintering were tested by turning test and compared with those of a conventional cemented carbide cutting tool. The results show that the cutting force, the friction coefficient of the rake face, and the wear of the GFCC cutting tool are lower than those of the conventional cutting tool with the same composition. Additionally, the effects of cutting speed on cutting force and tool wear were studied. Furthermore, the failure mechanism in the cutting process, the heat distribution of the second derformation zone and the resistant to the generation and extend of tool surface micro-cracks were analyzed. The friction and wear mechanism of the FGCC tool was found to be affected by the gradient distribution of the tool surface composition.

Keywords: Functional gradient tool; cemented carbide; microwave heating; cutting performance

***Corresponding Author: Siwen Tang:** Hunan Provincial Key Laboratory of Health Maintenance for Mechanical Equipment, Hunan University of Science and Technology, Xiangtan 411201, China; Email: siw_tang@hnust.edu.cn
Peizhen Li: Hunan Provincial Key Laboratory of Health Maintenance for Mechanical Equipment, Hunan University of Science and Technology, Xiangtan 411201, China
Deshun Liu: Engineering Research Center of Advanced Mining Equipment, Ministry of Education, Hunan University of Science and Technology, Xiangtan 411201, China
Pengnan Li, Qiulin Niu: Hunan Provincial Key Laboratory of High Efficiency and Precision Machining of Difficult-to-Cut Material, Hunan University of Science and Technology, Xiangtan 411201, China

1 Introduction

Cemented carbides are advanced composite materials made of WC-Co as the basic component, adding TiC, TaC, NbC, Mo_2C, and others prepared by mixing, pressing, and sintering: they have a high strength and hardness and have a wide range of applications in cutting tools, moulds, and drilling equipment, but its wear-resistant and heat-resistance in high-speed processing is limited [1, 2]. Formation of a wear-resistant layer (fcc-enriched) on the surface of the cemented carbide by nitriding to form a functionally graded carbide (FGCC) can effectively improve the cutting performance of the tool [3–8]. Barbatti *et al.* [9] compared the cutting performance of the tools fabricating by nitriding and vacuum sintering. It was found that the wear resistance of the gradient alloy sintered by nitriding was three times than that of the homogeneous tool fabricated by vacuum sintering. Numora *et al.* [3] compared the cutting performance of fcc-enriched functionally graded cemented carbide and a homogeneous cermet tool used to cut an SCM435 steel. The results show that the wear resistance of the functionally graded cemented carbide is about twice that of the cermet. Dreyer *et al.* [10] showed that the crater wear and flank wear of the functional gradient tool was, after nitriding, significantly lower than that of the homogeneous tool originally formed from the same raw material. Lengauer *et al.* [11] studied the cutting performance of gradient cemented carbide with different gradient layer thicknesses: the results show that the functional gradient cemented carbide with a 7 μm-thick gradient layer offers good cutting performance. However, the aforementioned functionally graded cemented carbides are all prepared by conventional heating nitriding, and the energy consumption therein is large and the process is time-consuming. Microwave heating was widely used in the preparation of ceramic materials with the advantages of volume heating, rapidity of heating, selectivity of heating, and improvements in the performance of materials among other characteristics [12, 13]. The authors have studied the effects of sintering process parameters on the mechanical properties

and the formation of the gradient layer prepared by microwave heating and nitriding: the results show that microwave heating nitriding can obtain fcc-enriched material on the functionally graded cutting tool surface in a very short time [14–16]. On that basis, the cutting performances of gradient cemented carbide tool fabricated by microwave heating were studied. In addition, the wear resistant mechanism of the tool is discussed.

2 Experimental methods and processes

The functional gradient cemented carbide tool material FGCC-T15 was prepared by the method reported elsewhere [15] with the raw material composition of 79wt% WC, 15wt% TiC and 6wt% Co at the sintering condition of 1430°C for 15min. In addition, the gradient layer structure of the gradient cemented carbide tool was shown in [15]. Dry turning tests were carried out on a LBR-370 CNC with a blade of SPUN1604EDFR-type, and the work-piece material was a quenched and tempered 40Cr. The cutting speed v_c was between 70 m/min and 350 m/min, the feed rate f was 0.1 mm/r, and the cutting depth a_p was 0.2 mm. The working cutting edge angle of the tool is 75 degrees during cutting. A dynamometer system comprised a Kister 9527B-type three-way piezoelectric dynamometer, a 5080-type charge amplifier, a PCIM-DAS1602/16-type data acquisition card, and a Dyno Ware System data acquisition system, and the three directional turning forces in the X-, Y-, and Z-axes was measured. During, and after, the cutting process, the wear morphology of the rake and the flank of the tool were measured and analysed by an ultra depth of field 3d microscope (Keyence VHX-500FE) and a scanning electron microscope (SEM) with energy dispersion spectrum (EDS) facility attached (JEOL 6390LV).

3 Experimental results

3.1 Cutting force

Figure 1 shows the three-way cutting force of gradient carbide cutting tool (FGCC-T15) when cutting, with a quenching and tempering 40Cr workpiece. As a comparison, the cutting force of a commercial traditional carbide cutting tool (YT15) with the same composition is shown. With the increase of cutting speed, the three-way cutting force of the FGCC-T15 tool first decreases and then increases. The main

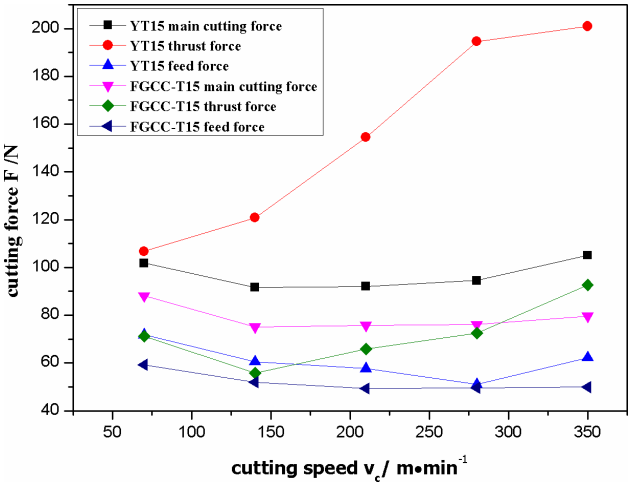

Figure 1: Cutting force exerted by the FGCC-T15 and YT15 tools

cutting force and feed force changes are small, however, the thrust force increases with increasing cutting speed. The trend in the main cutting force and feed force of the YT15 tool are the same as those of the FGCC-T15 variant, but the thrust force increases monotonically with the increase in cutting speed, and the rate of increase is much higher than that observed when using the FGCC-T15. The sharpness of the tool during cutting exerts a significant influence on the removal of and cutting force on the material. As the cutting speed increases, the beating of the workpiece increases. Since the edge of the FGCC-T15 tool is sharper than that on the YT15, its thrust force increases less, while, when using the YT15 tool, the thrust force increases to a significant extent.

3.2 Friction coefficient of rake face

The friction coefficient of oblique cutting can be calculated as follows:

$$\mu = \frac{F_{rf}}{W} = \frac{[A^2 + B^2]^{1/2}}{F_x \cos\gamma_n \sin i + F_y cos\gamma_n \cos i + F_z \sin\gamma_n} \quad (1)$$

$A = (F_x \cos i - F_y \sin i)$

$B = (-F_x \sin i \sin\gamma_n - F_y \cos i \sin\gamma_n + F_z \cos\gamma_n)$

Where: F_{rf} is the friction force of rake face, W is the positive pressure of rake face, they are all derive from the force in the work-piece coordinate system through the two coordinate system rotation. F_x, F_y, F_z are the feed force, main cutting force and thrust force in the work-piece coordinate system obtained from the dynamometer system, respectively. i is blade inclination. γ_n is the rake angle of the tool in the normal plane, its magnitude can be obtained by the tool

rake angle γ_0 as follows:

$$\tan \gamma_n = \tan \gamma_0 \cos i \quad (2)$$

where $i = \gamma_0 = -6°$.

The friction coefficient between the tool and the chip varies with the cutting speed as shown in Figure 2: with increased cutting speed, the friction coefficient of the FGCC-T15 tool decreases firstly and then increases, however, the friction coefficient of the YT15 tool first increases and then decreases. Overall, friction coefficient of FGCC-T15 changed slightly, but that of YT15 changed much more. The reason for the large changes in the friction coefficient is related to the increase in the thrust force on the YT15 tool and its increase with increased cutting speed.

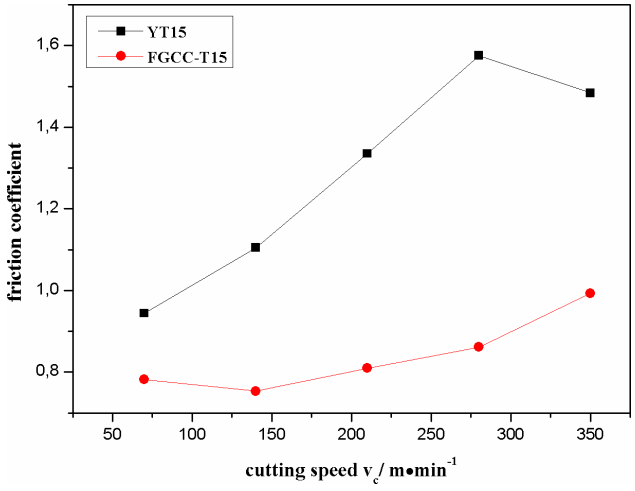

Figure 2: The friction coefficient between the tool and the chip varies with the cutting speed

3.3 Tool wear

3.3.1 Wear curve

Figure 3 shows the flank wear curves of the FGCC-T15 tool when cutting with quenched and tempered 40Cr under the following conditions: v_c = 120 m/min, a_p = 0.2 mm, f = 0.1 mm/r, and v_c = 240 m/min, a_p = 0.2 mm, f = 0.1 mm/r. Additionally, the same cutting conditions were used to make a comparison with the commercially available YT15 tool. The wear of the FGCC-T15 tool is low at low speed (v_c = 120 m/min), and the flank wear of the tool VB is still less than 0.1 mm after cutting for 100 min, far from ISO recommended blunt standard of VB = 0.3 mm. The FGCC-T15 tool wear has obvious three-stage wear characteristics at

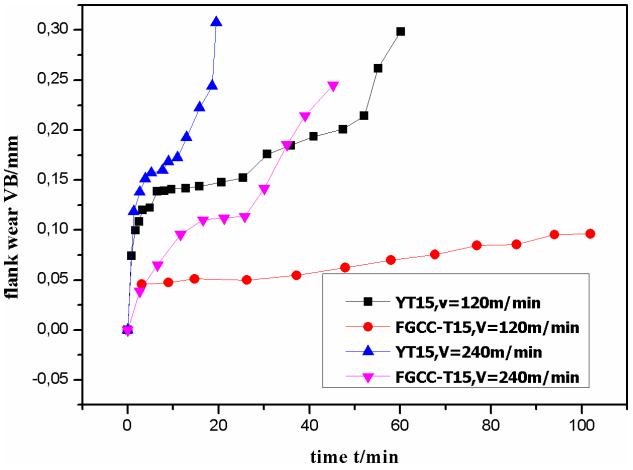

Figure 3: Wear curve of the gradient carbide tool

high speed (v_c = 240 m/min). The flank wear increased slowly at 0.1 mm or so, and there is a clear platform period. When the tool flank wears VB before and after 0.1 mm was reached, the flank wear became more rapid. The tool life of the FGCC-T15 sample is greater than 50 min at high speed. As a comparison, YT15 tools were reached the ISO recommended blunt standard both at low speed and high speed, the tool life at low speed life is about 60 min, and that at high speed is about 20 min. Compared with the homogeneous YT15 tool, the tool life of the FGCC-T15 sample was greatly improved, and at low speed it increased by 67%, and at high speed it increased by 130%. It should be noted that the FGCC-T15 tool life expectancy at low speed is much higher than 67% from the trend of the wear curve. Therefore, the gradient tool prepared by rapid microwave heating nitriding sintering exhibited a better cutting performance than the homogeneous tool with its longer preparation time.

3.3.2 Wear morphology

Figures 4 and 5 show the wear morphologies of the FGCC-T15 and YT15 tools when cutting quenched and tempered 40Cr steel. The rake face of the functionally gradient cemented carbide tool FGCC-T15 and homogeneous carbide tool YT15 all showed crater wear under the prevailing experimental conditions. The flank wear of the FGCC-T15 tool is mainly due to the wear of the main flank face. The flank wear of the YT15 tool consists of main flank wear, secondary flank wear, and boundary wear. When the speed is 240 m/min, the flank face of the YT15 tool also shows signs of plastic deformation. This is because the cutting temperature increases as the cutting speed increases, and

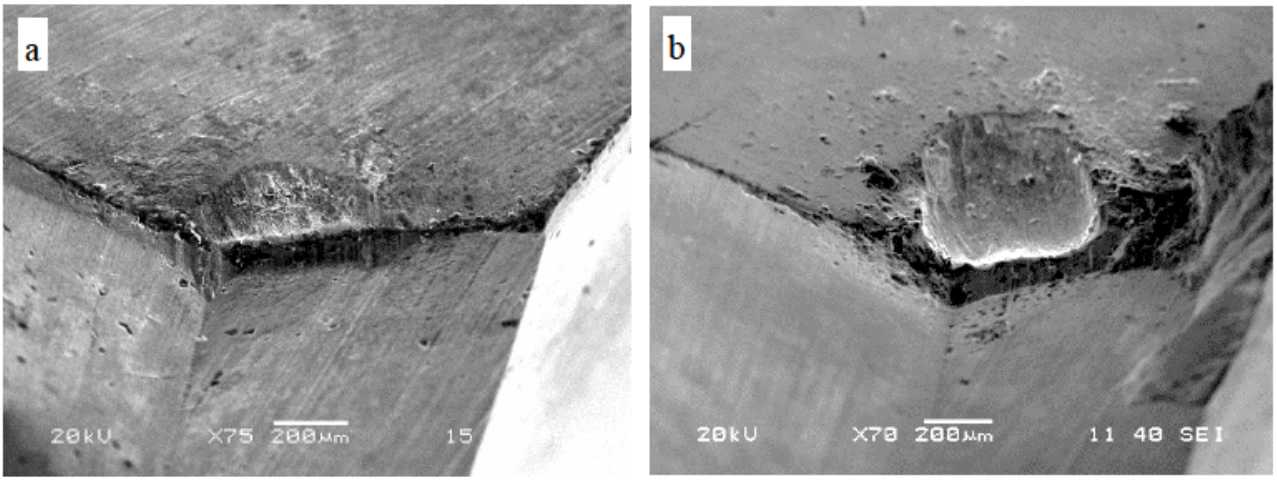

Figure 4: Wear morphology of the FGCC-T15 tool (a - v_c = 120 m/min, b - v_c = 240 m/min)

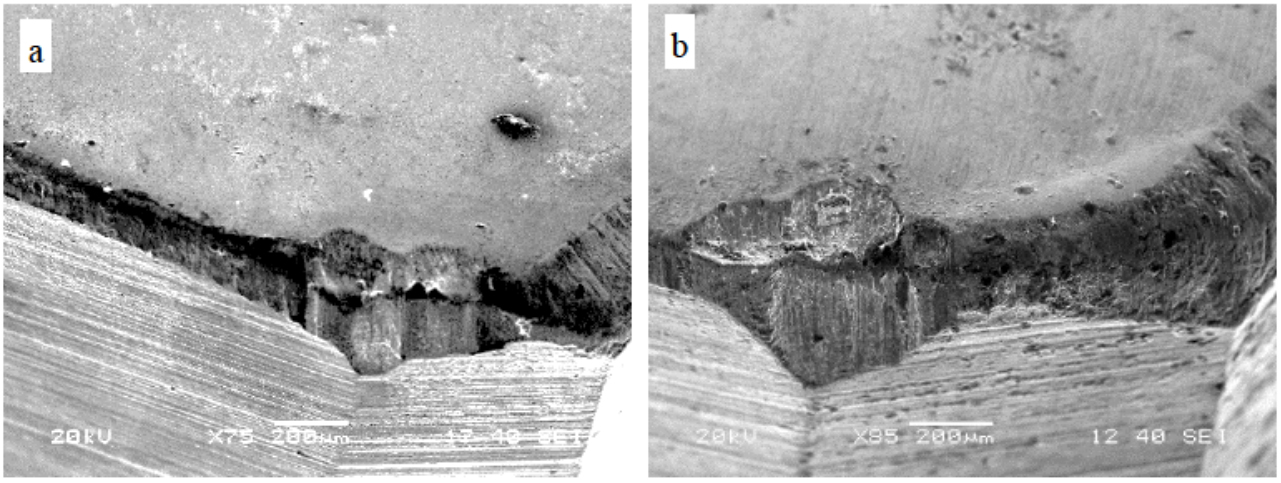

Figure 5: Wear morphology of YT15 tool (a - v_c = 120 m/min, b - v_c = 240 m/min)

the strength of the YT15 tool decreases and its plasticity increases at high temperatures. In addition, the plastic deformation could occur on the rear face under friction with the workpiece surface,however, there is no obvious plastic deformation feature observed on the rear face of the FGCC-T15 tool. This is because the FGCC-T15 tools have formed a TiCN-based surface [15], which has greater high-temperature hardness than that of a WC-based surface. It seems like there are some edge geometry discrepancy observed from the SEM images shown in Figure 4 and 5, and it probably due to the sample position with respect to the SEM.

Figures 6 and 7 show the wear morphologies of rake face of the FGCC-T15 and YT15 tools at different cutting speeds. Figures 6(a), 6(c) and 7(a), 7(c) show that the wear area and the depth of the crater wear of the two tools increases with increasing cutting speed. In contrast, the FGCC-T15 tool undergoes wider and smoother crater wear, and the YT15 tool has a deeper wear crater. From Figures 6(b), 6(d) and 7(b), 7(d), it can be seen that there are different degrees of adherence in the crater wear of the two kinds of tools. In addition to a large number of adhesive particles, there are some tiny chips and a large number of micro-cracks in the crater formed by the YT15 tool at high-speed (v_c = 240 m/min).

Figures 8 and 9 show the energy spectral analysis (EDS) data of the flank wear surface of the two kinds of cutting tools (FGCC-T15 and YT15). In contrast, the Fe and O contents of the flank surface of YT15 are higher than that of FGCC-T15, however, the Ti and W contents are lower. It can be inferred that the flank surface bonding and oxidation of YT15 was more severe and this indicates that the TiCN-based functionally graded tool has a lower affinity to Fe and is more difficult to bond.

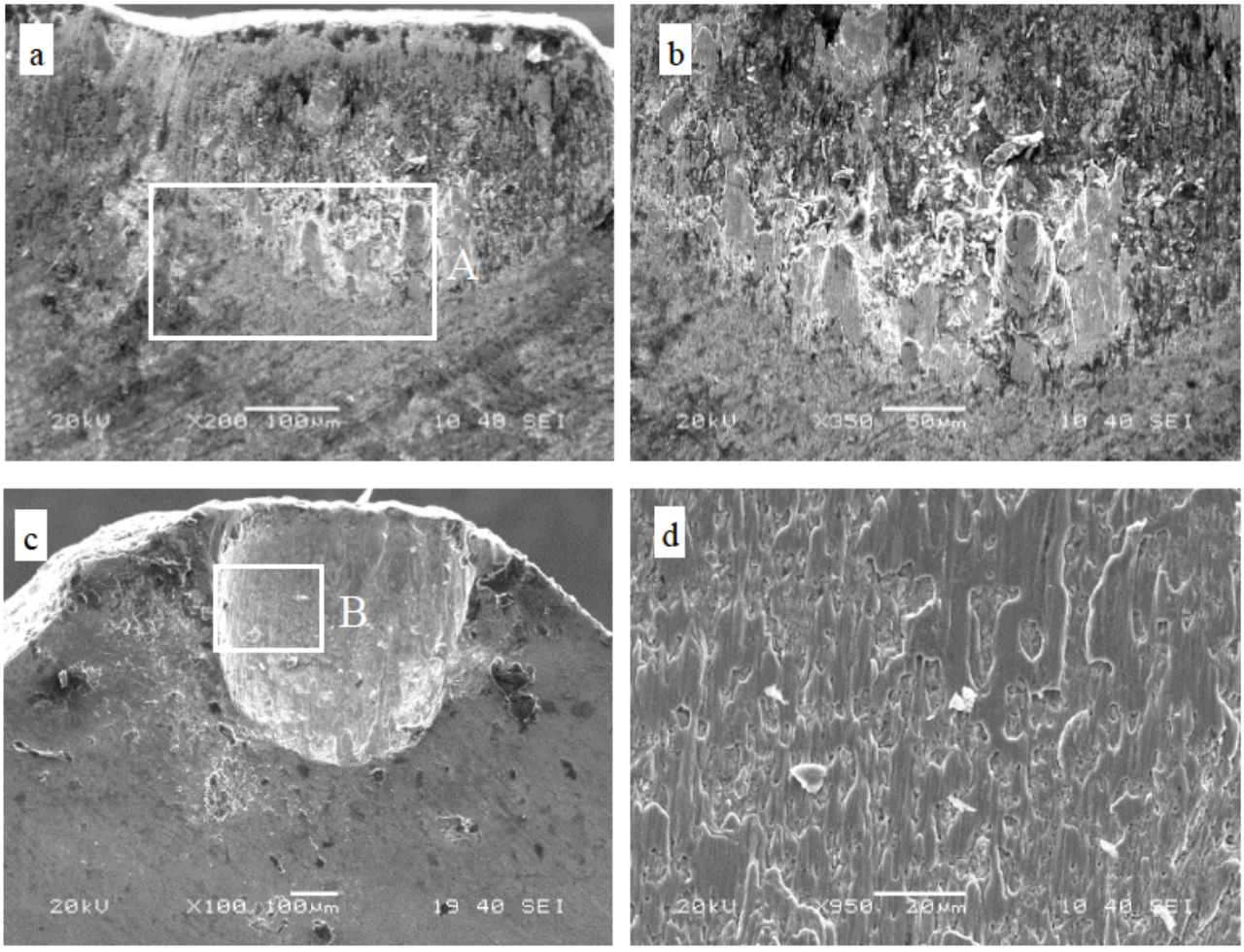

Figure 6: Rake face wear morphology of the FGCC-T15 tool (a - v_c = 120 m/min, b - enlarged view of area A, c - = 240 m/min, d - enlarged view of area B)

4 Discussions

4.1 Effect of gradient surface on cutting force

Cutting force is the resultant force used to overcome the separation of the workpiece and the force resulting from friction between tool and chips and between tool and workpiece. Friction between the tool and the chips, and tool and its workpiece, play a key role in the magnitude of the cutting force in the case of identical workpiece materials, especially that between tool and chip. The friction coefficient of the tool rake face in Figure 2 shows that the friction coefficient of FGCC-T15 is much lower than that of the YT15 tool, therefore, the cutting force exerted by the FGCC-T15 tool is correspondingly lower than that on the YT15 tool. From the perspective of the tool material, since the FGCC-T15 tool forms a surface layer with TiCN-Co as the main component [15], its friction coefficient is lower than that of WC-Co when coupled with steel because of the oxide production of TiCN being TiO_2, which played a role in the reduction in tool surface friction [17]. In addition, the contact area between the tool and the chip is generally considered to be divided into two areas of adhesion and sliding (named stick-slip friction in cutting), TiCN-Co is more efficient than WC-Co from the view of anti-adhesion, and it helps to reduce the friction and the cutting force. Moreover, TiCN-Co has a higher thermal stiffness than WC-Co and has better sharpness at high temperatures, and this is the reason why the YT15 tool thrust force increased significantly, while that on the FGCC-T15 tool changed little with increased speed.

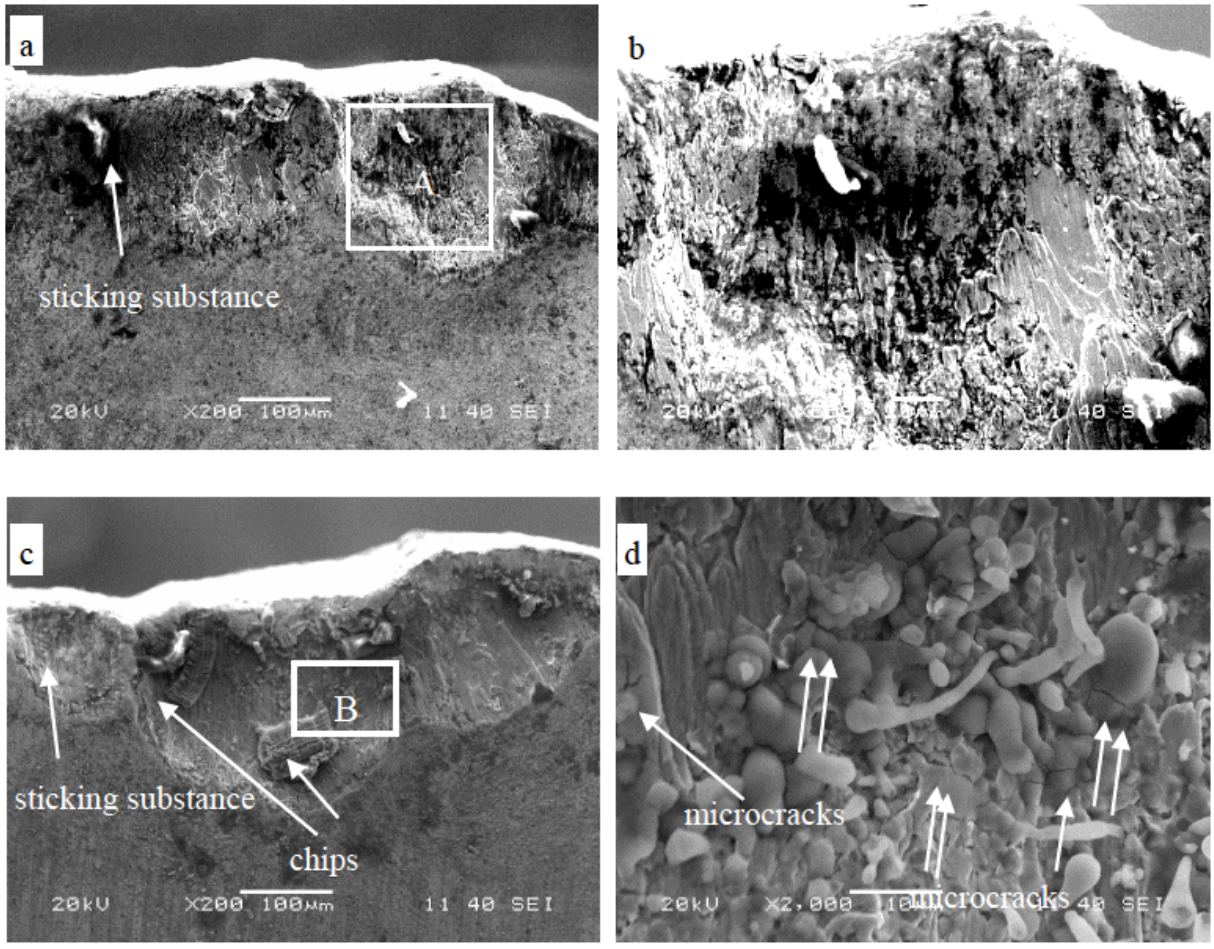

Figure 7: Rake face wear morphology of the YT15 tool v_c = 120 m/min, b - enlarged view of area A, c - v_c = 240 m/min, d - enlarged view of area B)

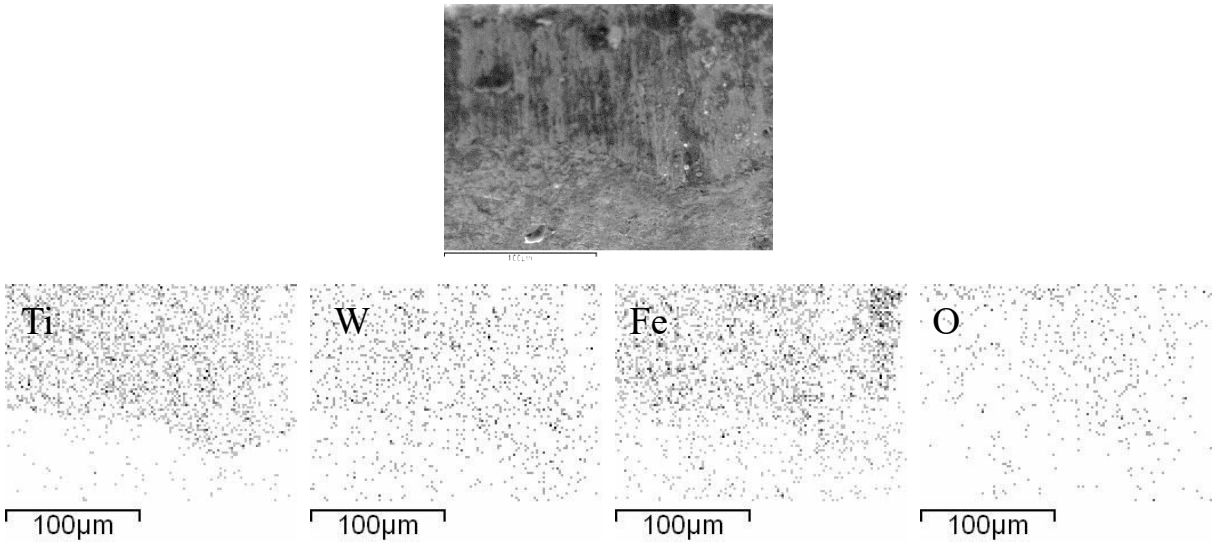

Figure 8: Energy spectrum analysis of flank wear of the FGCC-T15 tool (v_c = 120 m/min)

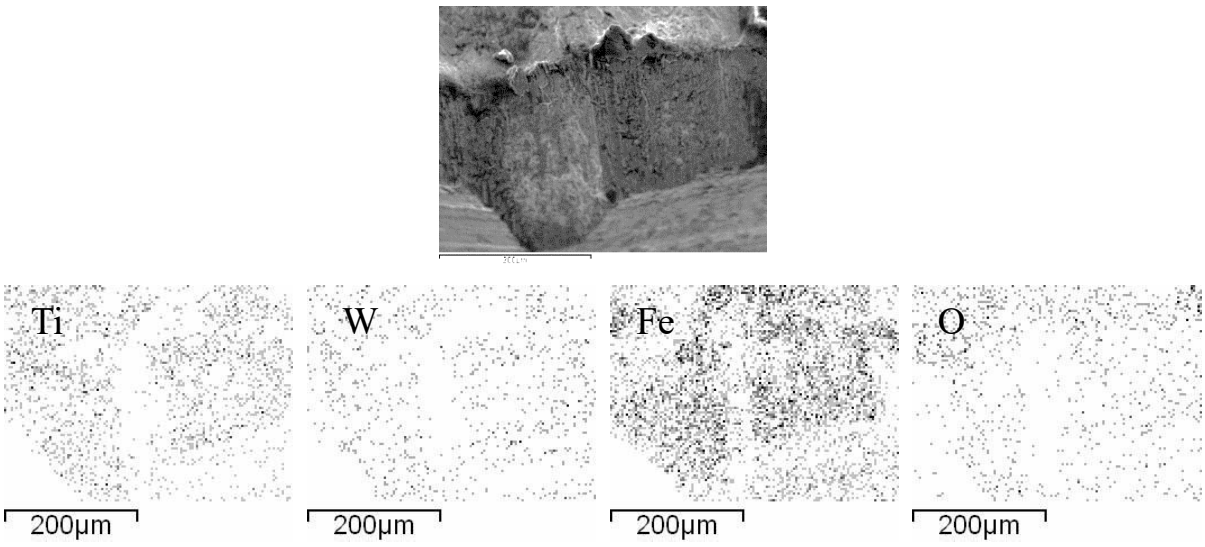

Figure 9: Energy spectrum analysis of flank wear of the YT15 tool (v_c = 120 m/min)

5 Effect of gradient surface on cutting heat distribution

Cutting temperature generally affects the cutting process. The cutting temperature generally refers to the average temperature of the contact area between the rake face and the chip. It can be approximated as the sum of the average temperature of the shear plane and the friction temperature of the tool-chip contact area. The TiCN-Co surface formed by gradient sintering helps to reduce the build-up of frictional heat. The decrease in frictional heat helps to reduce the heat generated under the same workpiece material conditions.

In terms of the distribution of cutting heat, the proportion of heat that flowed into the chip R_2 in the second deformation zone during the cutting process can be expressed as follows [18]:

$$R_2 = \frac{q_c}{q_t} = \frac{\sqrt{\rho_c k_c c_c}}{\sqrt{\rho_c k_c c_c} + \sqrt{\rho_t k_t c_t}} \tag{3}$$

Where, q_c is the heat that flowed into the chip as generated by the rake face, and q_t is the heat that flowed into the tool as generated by the rake face. In addition, ρ_c, K_c, and C_c are the density, heat transfer coefficient, and specific heat capacity of the chip, respectively; ρ_t, K_t, and C_t are the density, heat transfer coefficient, and specific heat capacity of the tool, respectively (these all change with temperature). Eq. (3) is transformed to obtain:

$$R_2 = \frac{q_c}{q_t} = \frac{1}{1 + \sqrt{\frac{\rho_t k_t c_t}{\rho_c k_c c_c}}} \tag{4}$$

In the case of workpiece material selection, reducing the product of the density, heat transfer coefficient, and specific heat capacity of the cutting tool surface material can reduce the heat flow into the tool surface, thereby reducing the thermal shock to the tool. On the other hand, the temperature increase on the tool surface ΔT is inversely proportional to the specific heat capacity of the tool C_t. When the specific heat capacity of the tool surface is large enough, the temperature of the tool surface is small when the same heat flows into the tool surface, so that the tool surface temperature can be reduced. The gradient tool has a surface with added TiCN and a small amount of Co as its main components, and the product of the density, thermal conductivity, and specific heat capacity of TiCN is much lower than that of the WC, however, its specific heat capacity is higher than that of WC, therefore, in the view of the generation and distribution of heat in the cutting process, the functionally graded design can reduce tool temperature, and then improve tool life.

5.1 Effect of gradient surface on tool wear

Generally, the wear rate (W) of a brittle material can be estimated by a mechanical property factor $K_{IC}^{-3/4} \cdot H^{-1/2}$ as given by the following wear equation [2]:

$$W \propto K_{IC}^{-3/4} \cdot H^{-1/2} \tag{5}$$

where K_{IC} is the fracture toughness and H is the hardness of material. We know that TiCN has a higher hardness and similar transverse rupture strength to WC which leads to the lower wear of the FGCC-T15 tool. In addition, the tool

is hit by the work-piece and chips at high speed during the cutting process, and it is thus easy to form micro-cracks on the tool surface. There are obvious micro-fractures in the crater of the conventional homogeneous tool; however, despite the longer cutting distance, there are no visible micro-cracks in the crater of the gradient tool. There are two reasons for their different performances: on the one hand, since the tool forms TiCN-Co as the main component of the tool surface, and Co is present in the sub-surface layer of the tool [15], and the toughness of the Co at the sub-layer play a role in hindering the generation of cracks. On the other hand, a residual compressive stress is formed on the tool while forming the gradient surface, and its value is about 500 to 600 MPa [19], which has played an important role in hindering the expansion of the tool cracks formed in the cutting process [20]. Therefore, the wear resistance of FGCC is higher than that of a homogenous YT15 tool.

6 Conclusions

The cutting performance of functionally graded carbide cutting tools prepared by microwave heating and nitriding was investigated by means of a turning experiment. The main conclusions are as follows.

1) The three-way cutting force, and the friction coefficient, of an FGCC-T15 tool show a tendency to first decrease, and then decrease with increasing cutting speed.
2) Compared with the homogeneous tool initially made with the same material, the cutting force, the friction coefficient of the rake face, and the flank wear of the functional gradient tool are reduced to some extent. The tool life of gradient tool increased by more than 67% at low speed cutting compared to that of the homogeneous tool, while it increased by 130% at high speed cutting.
3) The reduced cutting force and improved tool life benefited from the gradient distribution of the FGCC tool surface composition which results in reduced friction, decreased heat distribution of the cutting tool, and the resistant to the generation and extend of the tool surface micro-cracks.

Acknowledgement: This work was financially supported by the National Natural Science Foundation of China (grant nos. 51305134 and 51605161), and National Green Manufacturing System Integration Project (2017), and a Foundation of Hunan University of Science and Technology (grant no.E56128).

References

[1] H. Zhang, J. Yan and X. Zhang, et al, Int. J. Refract. Met. H., 24 (2006) 236-239.
[2] H. Zhang, S. Tang, J. Yan and X. Hu, Int. J. Refract. Met. H., 25 (2007) 440-444.
[3] K. Tsuda, A. Ikegaya, K. Isobe, et al, Powder. Metall., 39 (1996) 296-300.
[4] T. Nomura, H. Moriguchi, K. Tsuda, et al, Int. J. Refract. Met. H., 17 (1999) 397-404.
[5] V. Ucakar, K. Dreyer and W. Lengauer, Int. J. Refract. Met. H., 20 (2002) 195-200.
[6] L. Chen, W. Lengauer, K. Dreyer, Int. J. Refract. Met. H., 13 (2000) 343-351.
[7] L. Chen, W. Lengauer, P. Ettmayer, et al, Int. J. Refract. Met. H., 18 (2000) 307-322.
[8] W. Lengauer and K. Dreyer, Jalloy., 338 (2002) 194-212.
[9] C. Barbatti, J. Garcia, F. Sket, et al, Surf. Coat. Tech., 202 (2008) 5962-5975.
[10] K. Dreyer, D. Kassel, H. W. Daub, Proceedings of the XV International Conference on Functionally Graded Hardmetals,Cermets Preparation, Performance and Production Scale Up, (2001), pp. 768-782.
[11] W. Lengauer and K. Dreyer, Int. J. Refract. Met. H., 24 (2006) 155-161.
[12] D. Demirskyi, A. Ragulya and D. Agrawal, Ceram. Int. 37 (2011) 505-512.
[13] R. Bao and J. Yi, Int. J. Refract. Met. H., 43 (2014) 269-275.
[14] S. Tang, D. Liu, P. Li, et al, Int. J. Refract. Met. H., 48 (2015) 217-221.
[15] S. Tang, D. Liu, P. Li, et al, Int. J. Refract. Met. H., 58 (2016) 137-142.
[16] S. Tang, D. Liu, P. Li, et al, High. Temp. Mat. Pr-isr., 34 (2015) 457-460.
[17] A. Erdemir, Tribol. Lett., 8 (2000) 97-102.
[18] E. G. Ng, D. K. Aspinwall, D, Brazil, et al, Int. J. Mach. Tool. Manu., 39 (1999) 885-903.
[19] C. Su, D. Liu, S. Tang, et al, High. Temp. Mat. Pr-isr., In press.
[20] T. Nomura, H. Moriguchi, K. Tsuda, et al, Int. J. Refract. Met. H., 17 (1999) 397-404.